Flux dependence of cluster formation in neutron irradiated weld material – Small-angle neutron scattering experiments and rate theory simulation

Frank Bergner, Uwe Birkenheuer, Andreas Ulbricht, and Frank-Peter Weiss

***Abstract*–Small-angle neutron scattering was applied to investigate the size distribution of irradiation-induced defect-solute clusters in a reactor pressure vessel weld material containing 0.22 wt% copper. In order to identify flux effects the material was exposed to neutron irradiations at two different levels of neutron flux in such a manner that the same value of neutron fluence was accumulated. We observed a pronounced effect of neutron flux on the cluster size, whereas the total volume fraction of the irradiation-induced clusters was found to be insensitive to the level of flux. The result is compatible with a rate theory model according to which the range of applied fluxes covers the transition from a flux-independent regime at lower fluxes to a regime of decelerating cluster growth. The issue of the effect of flux on the mechanical properties is also addressed.**

I. Introduction

THE core-belt region of the reactor pressure vessel (RPV) of a nuclear power plant (NPP) is exposed to intense neutron irradiation, the fast neutrons causing a degradation of the mechanical properties. In order to guarantee the structural integrity of the RPV throughout the operation time, surveillance programmes were implemented prior to initial commissioning of an NPP. According to these programmes specimens of the RPV steel were inserted into capsules and placed in special surveillance channels. At these positions the fast neutron flux is higher than the flux at the RPV wall by a leading factor (typically between 1.5 and 12). The specimens are taken from the surveillance capsules at regular intervals in order to undergo mechanical tests. The mechanical properties are then assumed to be characteristic of the RPV material at an instant of time corresponding to the irradiation time of the specimen multiplied by the leading factor. However, this procedure is only applicable, if flux effects are either completely absent, i.e. the degradation depends on fluence only, or result in a conservative prediction of the behaviour of the RPV material. At this point the basic interest in the dependence of the mechanical property changes and the underlying microstructural processes on neutron flux becomes evident.

The flux dependence of the microstructure and the mechanical properties of RPV steels and related model alloys is still an unresolved issue [1], [2]. Flux effects also depend on chemical composition. For pure Fe under irradiation, the balance equation for single vacancies combines a generation term, which is proportional to flux, a term describing the recombination of vacancies with self-interstitial atoms (SIA) and a sink term. The discussion of both the flux dependence of the steady state vacancy concentration and the vacancy-assisted diffusion of Cu shows that flux independence of the microstructure is expected at lower fluxes and a pronounced dependence of the microstructure on flux is expected at higher fluxes. If flux approaches zero, the vacancy concentration in thermal equilibrium can no longer be ignored in comparison with the steady state concentration introduced above. This effect gives rise to another kind of flux dependence (thermal regime). In the other extreme, at highest fluxes the irradiation time needed in order to accumulate a given neutron fluence no longer allows the steady state vacancy concentration to be reached.

In this contribution, small-angle neutron scattering was applied to investigate the size distribution of irradiation-induced solute clusters in an RPV weld material of a relatively high level of impurity Cu (0.22 wt%). While the material was exposed to neutron irradiations at two different levels of neutron flux, the same value of neutron fluence was accumulated in both cases in order to separate the flux effect. The observed microstructures are confronted with results of rate theory simulations on the one hand and with experimentally obtained irradiation-induced changes of mechanical properties on the other hand.

II. Experiments

The material investigated is a first generation submerged weld NiCrMo1 UP (modified)/ LW320, LW340 (German specification) containing an impurity Cu level of 0.22 wt%. The composition is given in Table I, the irradiation conditions are summarized in Table II and the irradiation-induced mechanical property changes are compiled in Table III. Slices of cross-sectional area of 10 x 10 mm and of 1 mm thickness were prepared for the small-angle neutron scattering (SANS) experiment.

Manuscript received November 14, 2008. This work was supported in part by the German Bundesministerium für Wirtschaft under Grant No. 1501315.

F. Bergner is with the Institute of Safety Research at Forschungszentrum Dresden-Rossendorf, 01314 Dresden, Germany (telephone: +49-351-2603185, e-mail: f.bergner@fzd.de).

U. Birkenheuer is with the Institute of Safety Research at Forschungszentrum Dresden-Rossendorf, 01314 Dresden, Germany (telephone: +49-351-2602477, e-mail: u.birkenheuer@fzd.de).

A. Ulbricht is with the Institute of Safety Research at Forschungszentrum Dresden-Rossendorf, 01314 Dresden, Germany (telephone: +49-351-2603155, e-mail: a.ulbricht@fzd.de).

F.-P. Weiss is Head of the Institute of Safety Research at Forschungszentrum Dresden-Rossendorf, 01314 Dresden, Germany (telephone: +49-351-2603480, e-mail: f.p.weiss@fzd.de).

The SANS measurements were performed at the instrument V4 of the Hahn Meitner Institute Berlin [3]. The samples were placed in a magnetic field of 1.2 T perpendicular to the incident neutron beam. The beam diameter was 7.5 mm and the neutron wavelength was 0.6 nm. Two sample-detector distances of 1.1 m and 4 m were chosen, thus covering a range of scattering vectors, Q, from 0.2 to 3.0 nm^{-1}. The collimation length of the neutron beam was 2 and 4 m, respectively. The principle of a SANS experiment is schematically shown in Fig. 1. The raw-data treatment including transmission measurement and correction for both background and detector sensitivity is described in [4]. For absolute calibration the water standard was used. Data analysis including separation of magnetic and nuclear scattering cross-sections was performed using the BerSANS software package [5]. The incoherent scattering cross-sections were determined on the basis of Porod plots and subtracted from the total cross-sections. The unirradiated conditions for each material were taken as reference.

TABLE I
COMPOSITION OF THE INVESTIGATED MATERIAL (WT%, BALANCE FE)

C	Si	P	S	V	Cr	Mn	Ni	Cu	Mo
0.08	0.15	0.015	0.017	0.001	0.74	1.10	1.11	0.22	0.60

TABLE II
IRRADIATION CONDITIONS (FLUENCE AND FLUX VALUES FOR NEUTRON ENERGY, E > 1 MEV)

Code	Fluence (cm^{-2})	Flux ($cm^{-2}s^{-1}$)	Time	Temperature (°C)
I-1 (high flux)	2.2×10^{19}	2.1×10^{12}	122 days	285
I-2 (low flux)	2.2×10^{19}	6.0×10^{10}	11.6 years	288

TABLE III
IRRADIATION INDUCED CHANGES OF YIELD STRESS, σ_y, AND BRITTLE-DUCTILE TRANSITION TEMPERATURE, T_{41}

Code	$\Delta\sigma_y$ (MPa)	ΔT_{41} (K)
I-1	211	119
I-2	196	111

Further analysis based on the indirect transformation method provides the size distribution of scatterers without assuming a certain type of distribution. The resolution limits of SANS for the present conditions are 0.5 nm and 0.005% with respect to the radius and to the total volume fraction of scatterers, respectively. According to our standard analysis [6]-[9] we have assumed that the system consists of isolated scattering particles in a homogeneous matrix (two-phase approach) and that the particles are spherical and non-magnetic. The A-ratio defined as ratio of the scattering cross-sections perpendicular and parallel to the magnetic field direction was calculated in the size space after performing the transformation according to the relation, $A=1+M/N$, where M and N denote the area under the size distribution curve obtained from the magnetic and nuclear scattering contribution, respectively.

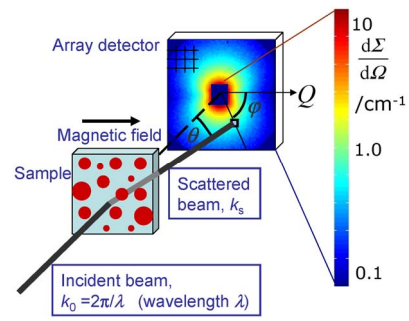

Fig. 1. Scheme of a SANS experiment. When a saturation magnetic field with the field direction oriented perpendicular to the incident neutron beam is applied to the sample, the intensity pattern of the array detector exhibits a characteristic anisotropy, which was used to separate magnetic and nuclear contributions to scattering.

III. RESULTS

The coherent magnetic scattering cross-section, $(d\Sigma/d\Omega)_{mag}$, obtained for the RPV weld material and the reconstructed size distribution of the irradiation-induced features are plotted in Fig. 2. The scattering cross-sections of the low- and high-flux irradiations exhibit characteristic differences manifesting themselves in different size distributions. The quantities characterizing the size distributions are summarized in Table IV.

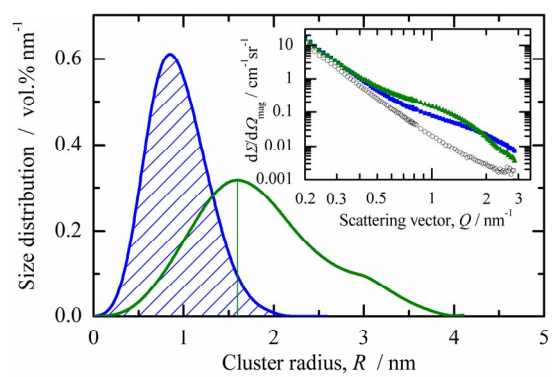

Fig. 2. Coherent magnetic scattering cross-sections, $d\Sigma/d\Omega$, obtained for the RPV weld material (see insert) and the reconstructed size distributions. The symbols and curves are related to the high-flux irradiation (blue), the low-flux irradiation (green) and the unirradiated reference (open circles). The total volume fraction of irradiation-induced scatterers and the peak radius of the size distribution are indicated by the hatched area and by the green line, respectively.

TABLE IV
CHARACTERISTICS OF IRRADIATION-INDUCED CLUSTERS DETECTED BY SANS

Code	Peak radius (nm)	Volume fraction (%)	Number density (cm^{-3})	A-ratio
I-1	0.85	0.51 ± 0.02	17×10^{17}	2.3 ± 0.1
I-2	1.6	0.53 ± 0.02	5×10^{17}	2.5 ± 0.1

IV. Discussion

A. SANS results

The increase of the size of the scatterers is the most prominent effect of reducing the flux by a factor of 35 at constant fluence. Both peak radius (Table IV) and maximum radius (Fig. 2) of the size distribution of scatterers for the RPV weld differ by a factor of about 2. The total volume fraction of scatterers is approximately independent of flux. The increase of size at constant volume fraction requires the number density to decrease as shown in Table IV.

We have observed that the *A*-ratio is approximately independent of flux. This is an indication of similar compositions and, therefore, similar SANS contrast of the average scatterers in both cases. The *A*-ratio of about 2.4 implies that the scatterers are not pure bcc Cu, which would require a much higher *A*-ratio [8]. This is confirmed by the measured total volume fractions, which are significantly larger than the maximum volume fraction of pure Cu clusters achievable due to the Cu content of the weld. In fact, 0.22 wt% Cu (Table I) have to be converted into 0.19 at% Cu and, taking into account the lattice constants of Fe and bcc Cu reported in [10] but neglecting misfit strain, into 0.21 vol% bcc Cu, i.e. much less than the measured fractions of 0.51 or 0.53 vol% (Table IV). Nevertheless, as it is well known from several studies of Cu-bearing RPV steels and model alloys (e.g. [2], [8], [9]), Cu is an important constituent of the scatterers and plays a decisive role in the formation process.

These results and the background presented in the introduction indicate that irradiation-enhanced Cu diffusion controlled by the vacancy concentration could be responsible for the observed flux effect. In order to check this possibility, we apply a rate theory approach below.

B. Rate theory modelling

The constituents of our rate theory model are (i) a set of two ordinary differential equations describing the temporal change of the concentration of point defects (vacancies and self-interstitial atoms), (ii) a set of ordinary differential equations describing the temporal change of the concentration of Cu-clusters containing a number of *N* Cu-atoms (*N* = 1 … 10000), and (iii) an assumption relating the ratio of irradiation-enhanced and thermal Cu-diffusivity to the ratio of steady-state and equilibrium concentration of vacancies.

The rates of change of the vacancy concentration, C_v, and the self-interstitial atom (SIA) concentration, C_i, are described by (1) and (2), respectively [11].

$$\frac{dC_v}{dt} = G_v - \frac{4\pi r(D_v + D_i)C_v C_i}{\Omega_a} - K_v C_v \quad (1)$$

$$\frac{dC_i}{dt} = G_i - \frac{4\pi r(D_v + D_i)C_v C_i}{\Omega_a} - K_i C_i \quad (2)$$

G_v and G_i are the production rates of free vacancies and free SIA due to neutron irradiation, $K_v = D_v S_v$ and $K_i = D_i S_i$ are rate constants, D_v and D_i are the diffusivities of vacancies and SIA, S_v and S_i are the sink strengths for vacancies and SIA, respectively. Ω_a is the atomic volume of iron and r is the recombination or trap radius. In the steady state, the left-hand sides of (1) and (2) vanish and the steady-state vacancy concentration, C_{vss}, can be expressed by solving a quadratic. We shall focus on the flux dependence here:

$$C_{vss} = 2.4 C_{vss,t}\left(\sqrt{1+\frac{\varphi}{\varphi_t}} - 1\right) \quad (3)$$

φ is the flux and φ_t is the value of the flux at the transition between two regimes of the flux dependence. $C_{vss,t}$ is the steady-state vacancy concentration at the flux, $\varphi = \varphi_t$. We have found that the steady-state vacancy concentration under the present irradiation conditions is orders of magnitude higher than the equilibrium concentration. It is concluded that the applied neutron flux in both irradiation conditions is well above the thermal regime mentioned in the introduction. We have also observed that the time required to reach the steady state is of the order of some hundreds of seconds, i.e. much less than the irradiation time. Therefore, further analysis is focussed on the two flux regimes resulting from the asymptotic behaviour of (3) with respect to flux.

The expression in parentheses is asymptotically proportional to φ for $\varphi << \varphi_t$ and to $\varphi^{1/2}$ for $\varphi >> \varphi_t$. φ_t is given by [2]:

$$\varphi_t = \frac{\Omega_a D_v S_v^2}{16\pi r \xi \sigma_{dpa}} \quad (4)$$

σ_{dpa} is the displacement-per-atom (dpa) cross-section and ξ is the fraction of vacancies and SIA created per dpa. Rate theory of the evolution of Cu clusters [12] shows that cluster growth is governed by the dimensionless parameter $D^*_{Cu} t / a^2$, where t is the irradiation time, D^*_{Cu} is the irradiation-enhanced diffusion coefficient of Cu in Fe and a is the lattice parameter of bcc Fe. We use the approximation [13]:

$$D^*_{Cu} = D_{Cu}\frac{C_{vss}}{C_{veq}} \quad (5)$$

Here D_{Cu} and C_{veq} are Cu diffusivity and vacancy concentration in thermal equilibrium, respectively. Therefore, we arrive at the conclusion that the cluster growth at a given value of fluence, ψ, is a monotonically decreasing function of flux and its behaviour is governed by the kinetics parameter, k, according to:

$$k = D^*_{Cu} t / \psi \sim \begin{cases} \text{constant} & \varphi << \varphi_t \\ 1/\sqrt{\varphi} & \varphi >> \varphi_t \end{cases} \quad (6)$$

The rate-theory model shows that the disappearance of vacancies is dominated by the loss in sinks such like

dislocations in the flux-independent low-flux regime. In the high-flux regime recombination with SIA is prevailing. An estimation of the transition flux, φ_t, using $S_v = 10^{14}$ m^{-2} (i.e. the order of magnitude of the dislocation density), D_v(285°C) = 10^{-16} m^2/s, r = 0.574 nm, ξ = 0.4 and σ_{dpa} = 1.5 x 10^{-25} m^2 [2] gives φ_t = 7 x 10^{11} cm^{-2}s^{-1}. The kinetics parameter, k, normalized with the flux-independent limit, k_0, at low fluxes is plotted in Fig. 3 as a function of the normalized flux, φ/φ_t. We expect the low-flux condition for the RPV weld (condition I-2 in Table II) to be in the flux-independent regime of cluster growth and the high-flux condition (condition I-1 in Table II) to be outside and to exhibit a noticeably slower cluster growth. This is what we have observed according to Table IV.

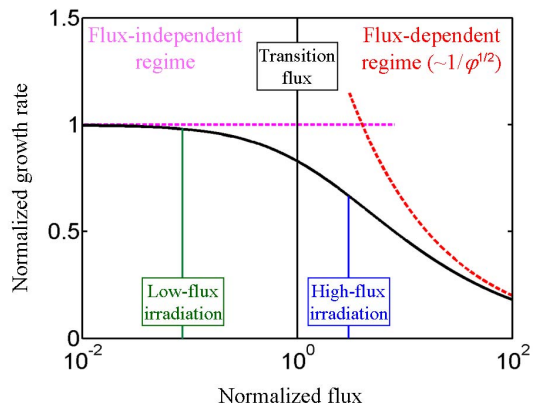

Fig. 3. Normalized growth parameter, k/k_0, versus normalized neutron flux, φ/φ_t. The exact solution (solid line) as well as the asymptotics (dashed lines) are shown. The value estimated for the transition flux according to (4) was used in order to convert the experimentally applied fluxes into normalized fluxes for both the high-flux (condition I-1) and the low-flux (condition I-2) irradiation.

In a more advanced version of our rate-theory model [14], [15], the Cu-clusters are explicitly considered as vacancy sinks in addition to the dislocation network. Then, the sets of rate equations describing point defects (i) and Cu-clusters (ii) are coupled because of the evolving sink term, S_v, in (1). Application of this approach allows to derive a quantitative estimation of the magnitude of the flux effect. We have found that the calculated flux effect on cluster size is much weaker than the measured one. Taking into account that only less than 50% of the total cluster volume fraction is occupied by Cu atoms, other components (not yet properly considered in our model) must also play a role. We ascribe the discrepancy to the contribution of alloying elements such as Mn and Ni to the cluster formation and growth.

C. *Microstructure versus mechanical properties*

In order to bridge the gap between nanoscale features and macroscopic mechanical properties, it is important to note that state-of-the-art models generally predict the materials resistance to plastic deformation (strength) to depend on both volume fraction and defect size [16]-[18]. Increase of strength in turn is correlated with the transition temperature shift [13]. Thus, our experimental findings, namely flux-dependence of cluster size (Table IV) and insensitivity of mechanical property changes to flux (Table III), rule out any model that predicts a pronounced size dependence of the transition temperature shift. The results substantiate the hypothesis that the mechanical properties are mainly determined by the total volume fraction of the defects, whereas the defect size seems to be of minor influence [7]. However, this hypothesis has to be underpinned by further studies.

V. Conclusions

SANS was applied to characterize the microstructure of an RPV weld material irradiated at neutron fluxes differing by a factor of 35 up to the same level of neutron fluence. We have observed that the size of the irradiation-induced clusters is two times larger on average for the irradiation at the lower flux, whereas both total volume fraction and average cluster composition turn out to be insensitive to flux.

Application of a rate theory model to the evolution of point defects and Cu-clusters shows that:

- The applied levels of neutron flux are well above the thermal regime and well below the transient regime.
- In between these limiting cases there is a flux-independent regime of cluster evolution, where the loss of vacancies in sinks is dominant, and a flux-dependent regime, where the loss of vacancies by recombination with interstitials is dominant.
- Estimation of the transition flux shows that the higher one of the two applied fluxes is in the flux-dependent regime, for which a decrease of the growth parameter as the inverse of the square root of flux is characteristic.
- This explains the presence and the direction of the observed flux effect on the cluster size.
- The coupled rate-theory model underestimates the magnitude of the observed flux effect.
- The discrepancy is ascribed to the observed presence of other solutes (Mn and Ni in particular) in the irradiation-induced clusters.

The observed insensitivity of mechanical property changes to flux rules out any model that predicts a pronounced size dependence of the transition temperature shift. Furthermore, the applicability of the surveillance procedure with respect to flux effects is confirmed in the present case.

Acknowledgment

We thank Hieronymus Hein for providing the neutron irradiated weld material with documentation and for helpful discussions as well as Martin Kammel for giving assistance at the SANS-facility at HMI Berlin.

References

[1] R. E. Stoller, "The Effect of Neutron Flux on Radiation-Induced Embrittlement in Reactor Pressure Vessel Steels," in *Effects of Radiation on Materials: 21st International Symposium* (ASTM STP 1447), M. L. Grossbeck, T. R. Allen, R. G. Lott and A. S. Kumar, Eds. West Conshohocken: ASTM International, 2003, pp 326-338.

[2] G. R. Odette, T. Yamamoto, and D. Klingensmith, "On the effect of dose rate on irradiation hardening of RPV steels," *Phil. Mag*., vol. 85 779–797, 2005.
[3] U. Keiderling and A. Wiedenmann, "New SANS Instrument at the BER II Reactor in Berlin", *Physica B*, vols. 213&214, pp. 895-897, 1995.
[4] P. Strunz, J. Saroun, U. Keiderling, A. Wiedenmann and R. Przenioslo, "General formula for determination of cross-section from measured SANS intensities," *J. Appl. Cryst.*, vol. 33, pp. 829-33, 2000.
[5] U. Keiderling "The new 'BerSANS-PC' software for reduction and treatment of small angle neutron scattering data" *Appl. Phys. A*, vol. 74, pp. S1455-S1457, 2002.
[6] A. Ulbricht, F. Bergner, C. D. Dewhurst and A. Heinemann, "Small-angle neutron scattering study of post-irradiation annealed neutron irradiated pressure vessel steels", *J. Nucl. Mater.*, vol. 352, pp. 233-240, 2006.
[7] A. Ulbricht, F. Bergner, J. Böhmert, M. Valo, M.-H. Mathon and A. Heinemann, "SANS response of VVER440-type weld material after neutron irradiation, post-irradiation annealing and reirradiation," *Phil. Mag.*, vol. 87, pp. 1855-1870, 2007.
[8] F. Bergner, A. Ulbricht, A. Gokhman and D. Erak, "Nature of defect clusters in neutron-irradiated iron-based alloys deduced from small-angle neutron scattering," *J. Nucl. Mater.*, vol. 373, pp. 199-205, 2008.
[9] F. Bergner, A. Ulbricht, H. Hein and M. Kammel, Flux dependence of cluster formation in neutron-irradiated weld material, *J. Phys.: Condensed Matter*, vol. 20, paper-ID 104262, 2008.
[10] G, J, Ackland, D. J. Bacon, A. F. Calder, and T. Harry, "Computer simulation of point defect properties in dilute Fe-Cu alloy using a many-body interatomic potential," *Phil. Mag. A*, vol. 75, pp. 713-732, 1997.
[11] L. K. Mansur, "Void swelling in metals and alloys under irradiation: An assessment of the theory," *Nucl. Technol.*, vol. 40, pp. 5-34, 1978.
[12] M. H. Mathon, A. Barbu, F. Dunstetter, F. Maury, N. Lorenzelli and C. H. De Novion, "Experimental study and modelling of copper precipitation under electron irradiation in dilute FeCu binary alloys, " *J. Nucl. Mater.*, vol. 245, pp. 224-237, 1997.
[13] G. R. Odette, "On the dominant mechanism of irradiation embrittlement of reactor pressure vessel steels," *Scr. Metall.*, vol. 11, pp. 1183-1188, 1983.
[14] A. Gokhman, F. Bergner, A. Ulbricht and U. Birkenheuer, "Cluster dynamics simulation of reactor pressure vessel steels under irradiation," *Defect and Diffusion Forum*, vol. 277, pp. 75-80, 2008.
[15] U. Birkenheuer, F. Bergner, A. Gokhman, A. Ulbricht and F.-P. Weiß, "Vacancy-coupled copper precipitation model for irradiated reactor pressure vessel steels", *J. Nucl. Mater.*, submitted.
[16] K. C. Russell, L. M. Brown, "A dispersion strengthening model based on differing elastic moduli applied to the iron-copper system," *Acta Met*,. vol. 20, pp. 969-974, 1972.
[17] D. J. Bacon, U. F. Kocks and R. O. Scattergood, "The effect of dislocation self-interaction on the Orowan stress," *Phil. Mag.*, vol. 28, pp. 1241-1263, 1973.
[18] S. Jumel, J.-C. Van Duysen, J. Ruste and C. Domain, "Interactions between dislocations and irradiation-induced defects in light water reactor pressure vessel steels," *J. Nucl. Mater.*, vol. 346, pp. 79–97, 2005.